Proc. Natl. Acad. Sci. USA
Vol. 93, pp. 3007–3010, April 1996
Biochemistry

The crystal structure of human glycosylation-inhibiting factor is a trimeric barrel with three 6-stranded β-sheets

(x-ray crystallography/multiple isomorphous replacement/α + β sandwich structure/cytokine)

YOICHI KATO*, TAKANORI MUTO*, TAKAFUMI TOMURA†, HARUHIKO TSUMURA†, HIROSHI WATARAI†, TOSHIFUMI MIKAYAMA†, KIMISHIGE ISHIZAKA‡, AND RYOTA KUROKI*§

*Central Laboratories for Key Technology, Kirin Brewery Company, Ltd., 1-13-5 Fukuura, Kanazawa-ku, Yokohama 236, Japan; †Pharmaceutical Research Laboratories, Kirin Brewery Company, Ltd., Souja-machi, Maebashi 371, Japan; and ‡La Jolla Institute for Allergy and Immunology, La Jolla, CA 92037

Contributed by Kimishige Ishizaka, December 11, 1995

ABSTRACT **Glycosylation-inhibiting factor (GIF) is a cytokine that is involved in the regulation of IgE synthesis. The crystal structure of recombinant human GIF was determined by the multiple isomorphous replacement method. The structure was refined to an *R* factor of 0.168 at 1.9 Å resolution. The overall structure is seen to consist of three interconnected subunits forming a barrel with three 6-stranded β-sheets on the inside and six α-helices on the outside. There is a 5-Å-diameter "hole" through the middle of the barrel. The barrel structure of GIF in part resembles other "trefoil" cytokines such as interleukin 1 and fibroblast growth factor. Each subunit has a new class of α + β sandwich structure consisting of two β-α-β motifs. These β-α-β motifs are related by a pseudo-twofold axis and resemble both interleukin 8 and the peptide binding domain of major histocompatibility complex protein, although the topology of the polypeptide chain is quite different.**

Glycosylation-inhibiting factor (GIF), is a 13-kDa cytokine involved in the formation of IgE-suppressive factor (1). GIF inhibits N-glycosylation of IgE-binding factors, and the unglycosylated IgE-binding factor then selectively suppresses IgE synthesis. Furthermore, GIF facilitates generation of antigen-specific suppressor T cells (2), and appears to be a subunit of antigen-specific suppressor T-cell factors (1). Indeed, the major cell source of GIF activity is antigen-specific suppressor T cells (3). After molecular cloning of GIF, however, it was found that various cell line cells contained 0.6-kb mRNA, which hybridized with GIF cDNA (4), and secreted the 13-kDa protein that reacted with polyclonal antibodies against recombinant GIF (5). Nevertheless, only the peptide from suppressor T cell had GIF bioactivity. More recent experiments provided evidence that the bioactive GIF and inactive GIF have an identical amino acid sequence and suggested that the bioactivity of GIF is generated by posttranslational modifications of the inactive protein (5, 6). Since neither N-glycosylation nor phosphorylation is involved in the generation of bioactive GIF, we speculated that the heterogeneity of GIF is a conformational transition of the protein (5). The present experiments were undertaken to determine the three-dimensional structure of recombinant human GIF in order to get an insight into the structural basis of its bioactivity. It was found that the crystal structure of GIF is a novel structure with a trimeric barrel with three 6-stranded β-sheets.¶

MATERIALS AND METHODS

Crystallization of GIF. The recombinant human GIF was expressed in *Escherichia coli* and was purified as described (6). GIF was crystallized by the hanging-drop vapor diffusion method. The protein solution was concentrated to 25 mg/ml using a centrifugal concentrator, Centricon-3 (Amicon). Droplets consisting of 5 μl of the protein solution and the same vol of 0.1 M Hepes buffer (pH 7.5) containing 2.0 M ammonium sulfate and 2% (wt/vol) polyethylene glycol 400 (Wako Pure Chemical, Osaka) were equilibrated against 1 ml of the same precipitating solution at 4°C. Polyethylene glycol 400 was necessary for reproductivity of GIF crystals. The crystals belong to the space group $P3_121$ with the unit cell dimensions $a = b = 96.6$ Å and $c = 105.8$ Å. There are three molecules in an asymmetric unit related by a noncrystallographic threefold axis.

Structure Determination. The crystal structure of GIF was determined by the multiple isomorphous replacement method. The diffraction data and phasing statistics are summarized in Table 1. Two different mercury derivatives suitable for structure analysis were obtained by the soaking method. Mercury chloride derivative was provided by soaking a crystal in 0.2 mM $HgCl_2$ for 5 days. Ethylmercurithiosalicylate (EMTS) derivative was prepared by soaking a crystal in 1.0 mM EMTS for 3 days. X-ray diffraction data of native GIF and its derivatives were collected with a Rigaku R-AXIS IIc imaging-plate diffractometer using one crystal. Heavy-atom positions from the difference Patterson and the difference Fourier maps were determined and confirmed using the vector verification program VERIFY (written by S. Roderick, Institute of Molecular Biology, University of Oregon). Refinement of heavy atom parameter and phase calculation at 2.8 Å resolution were executed using the program PHASES (7). The mean figure of merit about 11,969 reflections [$I > 3\sigma(I)$] was 0.49. The multiple isomorphous replacement electron density map was improved by the solvent flattening method (8) and the noncrystallographic symmetry averaging method with PHASES. Models were constructed using the program QUANTA (Biosym/MSI). The refinement was carried out by using the program X-PLOR (9). The resolution was extended step by step from 2.8 to 1.9 Å. The molecular model was corrected using $2F_o$-F_c map after each stage of refinement. Solvent molecules were identified at 1.9 Å resolution using QUANTA. The last step of structure refinement and the refinement of temperature factor were executed with the program TNT (10). The current *R* factor is 0.168 for 34,810 reflections with $F > 2\sigma(F)$. A Ramachandran plot shows all dihedral angles fall within normally allowed regions. The refinement statistics are summarized in Table 2.

The publication costs of this article were defrayed in part by page charge payment. This article must therefore be hereby marked "*advertisement*" in accordance with 18 U.S.C. §1734 solely to indicate this fact.

Abbreviations: GIF, glycosylation-inhibiting factor; EMTS, ethylmercurithiosalicylate; TIM, triosephosphate isomerase; MHC, major histocompatibility complex; IL, interleukin; FGF, fibroblast growth factor.

§To whom reprint requests should be addressed.

¶The atomic coordinates and structure factors have been deposited in the Protein Data Bank, Chemistry Department, Brookhaven National Laboratory, Upton, NY 11973 (reference 1GIF).

Table 1. Diffraction data and phasing statistics

	Native	$HgCl_2$	EMTS
Resolution, Å	1.9	2.5	2.7
Total observations	89,768	28,107	21,827
Unique reflections	34,810	15,887	10,192
Completeness, %	75.6	76.4	61.8
R_{merge}	0.060	0.066	0.083
R_{iso}		0.180	0.169
Heavy atom sites		2	3
R_{Cullis}		0.62	0.68
Phasing power		1.79	1.52
Mean figure of merit		0.49	

$R_{merge} = \Sigma_N\Sigma_n|I - \langle I\rangle|/\Sigma_{Nn}\langle I\rangle$, where N is the number of unique reflections, n is the number of multiple measurements of a particular reflection, I is the measured intensity of reflection, $\langle I\rangle$ is the average intensity of equivalent reflections. $R_{iso} = \Sigma|F_{PH} - F_P|/\Sigma|F_P|$, where F_{PH} is the derivative structure factor amplitude, F_P is the native structure factor amplitude. $R_{Cullis} = \Sigma\,||F_{PH} - F_P| - F_{H(calc)}|/\Sigma|F_{PH} - F_P|$, where F_{PH} is the derivative structure factor amplitude, F_P is the native structure factor amplitude, and $F_{H(calc)}$ is the calculated heavy atom structure factor. Summation is over the centric reflections only. Phasing power is the ratio of the rms heavy atom scattering factor amplitude to the rms lack of closure error.

RESULTS AND DISCUSSION

The overall structure of recombinant GIF is a trimer of the 13-kDa protein as shown in Fig. 1*A*. The trimer is in a barrel shape (25 Å radius and 30 Å long) formed by three β-sheets, and has a 5-Å-diameter hole through the middle. Some aromatic residues (three tyrosines and six histidines) were seen to be located in the hole region. Each β-sheet consists of six β-strands; four β-strands (β1, β2, β4, and β5) in a monomer and the other two β-strands (β3 and β6) from the adjacent subunits (Fig. 1*B*). Intermonomer interfaces were stabilized by the hydrophobic interaction involving aromatic residues. Six α-helices surround the outside of the barrel and are not involved in formation of the trimer. The structure somewhat resembles a barrel structure of triosephosphate isomerase (TIM barrel) (11). However, the overall topology is quite different. An eight-stranded TIM barrel is constructed from parallel β-strands (Fig. 2*B*), whereas GIF is constructed from three independent nonparallel β-sheets (Fig. 2*A*). The barrel structures with threefold symmetry are seen in the structures of tumor necrosis factor (13, 14) (Fig. 2*C*), β-prism structures (15, 16) (Fig. 2*D*), and trefoil cytokines (17–23). The structure of the GIF trimer seems to resemble trefoil cytokines such as interleukin 1 (IL-1) and fibroblast growth factor (FGF), although the whole structure of IL-1 and FGF (Fig. 2 *E* and *F*) is made up of a single polypeptide and all of the adjacent β-strands are antiparallel. It may be noted that all of GIF, IL-1, and FGF lack a signal peptide sequence but are secreted from mammalian cells through unknown mechanisms (4, 24, 25). Similarities in the barrel structures of the three proteins may suggest the possibility that a common or similar protein may associate with the molecules and facilitate their secretion. Furthermore, it appears that the structure of GIF trimer most resembles *Escherichia coli* signal transducing protein P_{II} (35). However, the biological significance cannot yet be determined from the similarity in structure between these proteins.

Table 2. Refinement statistics

Resolution range, Å	6.0–1.9
Protein atoms	2625
Water molecules	170
R factor, %	16.8
rms bond lengths, Å	0.018
rms bond angles, Å	3.035
rms dihedral angles	28.41
rms improper torsion	2.832

$R = \Sigma|F_o - F_c|/\Sigma|F_o|$, where F_o and F_c are the observed and calculated structure factors, respectively.

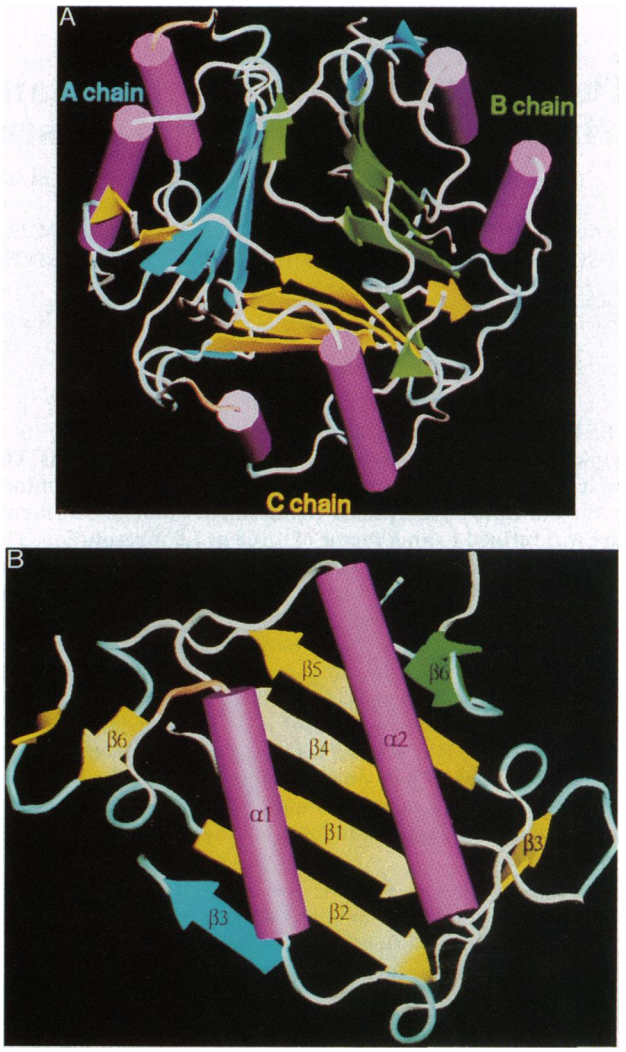

FIG. 1. (*A*) Schematic diagram of the GIF trimer. Cylinders in magenta represent α-helices and arrows in blue, green, and yellow represent β-strands from A, B, and C chains, respectively. (*B*) Schematic diagram of a GIF monomer (C chain). The α-helices are labeled as α1 and α2 and β-strands are labeled from β1 to β6. β2 of C chain (yellow) and β3 of A chain (blue) form an antiparallel β-sheet, and β5 of C chain and β6 of B chain (green) form an antiparallel β-sheet. Therefore, four strands of C chain (β1, β2, β4, β5) with β3 of A chain and β6 of B chain form one β-sheet.

The structure of the GIF monomer consists of two α-helices and a β-sheet as shown in Fig. 1*B*. The three monomers of GIF are similar to each other and can be superimposed within the difference RMS of 0.3 Å using C^α atom positions. Hydrophobic residues are packed between each α-helix and β-sheet. The distance between the center axes of two helices is ~12 Å and they are almost parallel to the threefold axis of the trimer. Two α-helices are located at the same side of the β-sheet and are related antiparallel to each other. This type of folding is classified as an α + β sandwich structure (26). The α + β sandwich structure of GIF is constructed from the repeat of β-α-β motifs (27) related by a pseudo-twofold axis located in the center of the monomer. Each β-α-β motif contains a parallel β-sheet. The whole sequence of the GIF monomer may be divided to two regions. The first half of the sequence contains residues 1–56 and the latter half contains residues 57–115. The common secondary structures (rectangles in Fig.

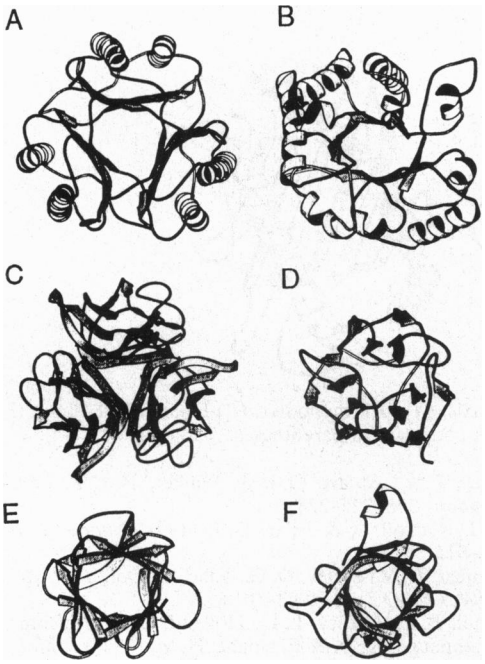

FIG. 2. Ribbon diagrams of several barrel structures. (*A*) GIF. (*B*) TIM barrel structure (3TIM). (*C*) Tumor necrosis factor α (1TNF). (*D*) β-prism structure of vitelline membrane outer layer protein I (1VMO). Trefoil cytokines of (*E*) FGF (4FGF) and (*F*) IL-1β (5I1B). Figures were drawn with the program MOLSCRIPT (12). Four-character codes in parentheses indicate entry code of the Protein Data Bank.

3*A*) located in the two regions were compared, showing a rms difference of ~1.4 Å (Fig. 3*B*). A weak sequence similarity was also detected between the two regions (Fig. 3*A*). The similar location of the intron determined by genomic DNA analysis (28) in this repeat suggests that this sequence repeat may be derived from gene duplication.

According to Orengo and Thornton (29), α + β sandwich structure can be further classified to a "split β-α-β fold" and "meander fold." The split β-α-β fold has a structure where another β-strand exists between two parallel β-strands of the β-α-β motif and forms an antiparallel β-sheet; the meander fold has an α + β sandwich structure with an antiparallel β-sheet and an α-helix. The meander fold is seen in the protein structures with immunological importance, such as IL-8 (Fig. 4*B*) and the peptide binding domain of major histocompatibility complex (MHC) proteins (Fig. 4*C*). Since GIF has a pseudo-twofold axis consisting of two β-α-β motifs having a parallel β-sheet, the topology of GIF is a new class of α + β sandwich structure. Comparison of the GIF structure to known proteins in the Protein Data Bank (release 70) using two programs, QUANTA/PROTEIN (Biosym/MSI) and COSEC (30), indicated that the structure of GIF is unique. Although the topology of the secondary structure of GIF does not resemble that of IL-8 or the peptide binding domain of MHC proteins, the overall structures of the three proteins are similar in outer appearance (Fig. 4).

The crystal structure of GIF may suggest possible conformational change of the helix region. The SH group of Cys-60, which is on the β4 strand located between the helices (cf. Fig. 1*B*) reacted with alkylating reagents such as iodoacetic acid and vinyl pyridine (data not shown). The relatively larger *B* values, which are often used as a scale of conformational flexibility, seen in the helix and adjacent loop regions may also indicate possible conformational changes. In mammalian cells, it is quite possible that a peptide or lipid is associated with GIF. Previous experiments have shown that bioactive GIF secreted from murine suppressor T-cell hybridomas bound to polyclonal and monoclonal antibodies specific for the I-J antigenic determinant (3, 31), which was originally considered to be encoded by a subregion of MHC (32, 33). However, molecular cloning of the MHC revealed that the I-J gene does not exist in the MHC subregion (34). Nevertheless, our recent experiments confirmed association of the I-J determinant with bioactive murine GIF. It was found that even bioactive human GIF secreted from a stable transfectant of human GIF cDNA in a H-$2^{b/d}$-derived murine suppressor T-cell hybridoma possesses an I-J^{b} determinant, while bioactive human GIF formed by a transfectant in monkey kidney cells lacked the determinant (6). These results indicate that the I-J phenotype of GIF is determined by the cells involved in posttranslational modification of the protein rather than its amino acid sequence. It is difficult to believe that H-2^{b} suppressor T cells and H-2^{k}-

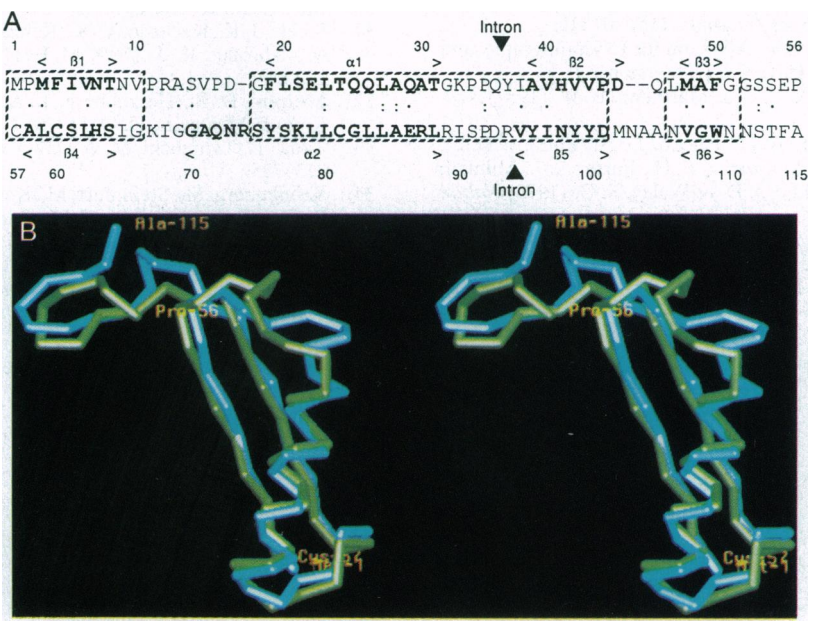

FIG. 3. (*A*) Sequence alignment of the N-terminal half (residues 1–56) to the C-terminal half (residues 57–115). Secondary structure parts are shown in boldface. Arrowheads represent locations of introns. Common structure elements used for superposition are surrounded by broken line. (*B*) Superposition of the C-terminal half onto the N-terminal half using the regions surrounded by the broken line in *A*.

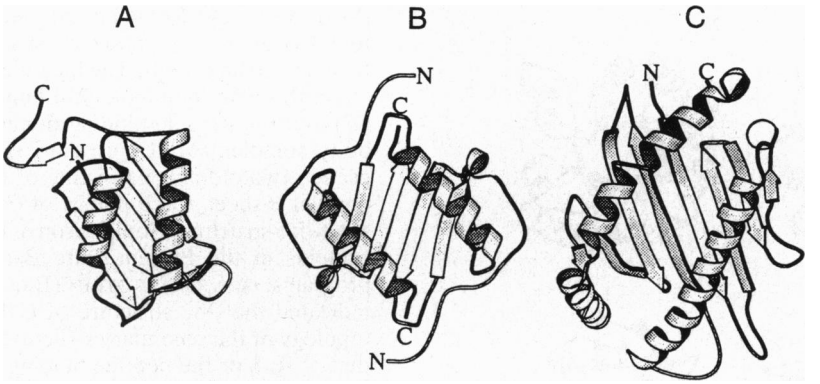

FIG. 4. Ribbon diagram of $\alpha + \beta$ sandwich structures having a pseudo-twofold axis. (*A*) GIF monomer. (*B*) Human IL-8 dimer (3IL8). (*C*) Peptide binding domain of human class I MHC protein (3HLA). Protein Data Bank codes are in parentheses.

derived suppressor T cells provide distinct conformational changes to GIF. However, the tertiary structure of GIF revealed in the present experiments raised the possibility that a substance such as a self peptide or lipid may be incorporated in the groove between the mobile α-helices and participate in the I-J epitope.

The authors express great appreciation to Drs. R. H. Jacobson, L. H. Weaver, and B. W. Matthews at the Institute of Molecular Biology, University of Oregon, for helpful advice on the structural determinations. We thank Dr. Shimizu for data collection, Drs. M. Kusunoki and T. Tsukihara for advice on the molecular averaging technique, and Mr. K. Kinoshita and Dr. N. Go for investigation of the GIF structure by the program COSEC.

1. Ishizaka, K. (1984) *Annu Rev. Immunol.* **2,** 159–182.
2. Iwata, M. & Ishizaka, K. (1988) *J. Immunol.* **141,** 3270–3277.
3. Jardieu, P., Akasaki, M. & Ishizaka, K. (1987) *J. Immunol.* **138,** 1494–1501.
4. Mikayama, T., Nakano, T., Gomi, H., Nakagawa, Y., Liu, Y.-C., Sato, M., Iwamatsu, A., Ishii, Y., Weiser, W. Y. & Ishizaka, K. (1993) *Proc. Natl. Acad. Sci. USA* **90,** 10056–10060.
5. Liu, Y.-C., Nakano, T., Elly, C. & Ishizaka, K. (1994) *Proc. Natl. Acad. Sci. USA* **91,** 11227–11231.
6. Nakano, T., Liu, Y-C., Mikayama, T., Watarai, H., Taniguchi, M. & Ishizaka, K. (1995) *Proc. Natl. Acad. Sci. USA* **92,** 9196–9200.
7. Furey, W. & Swaminathan, S. (1990) *PA33 Am. Crystallogr. Assoc. Meeting Abst. Ser. 2* **18,** 73.
8. Wang, B. C. (1985) *Methods Enzymol.* **115,** 90–112.
9. Brünger, A. T. (1992) X-PLOR: A System for Crystallography and *NMR* (Yale Univ., New Haven, CT), Version 3.1.
10. Tronrud, D. E., Ten Eyck, L. F. & Matthews, B. W. (1987) *Acta Crystallogr* **43,** 489–503.
11. Banner, D. W., Bloomer, A. C., Petsko, G. A., Phillips, D. C., Pogson, C. I., Wilson, I. A., Corran, P. H., Furth, A. J., Milman, J. D., Offord, R. E., Priddle, J. D. & Waley, S. G. (1975) *Nature (London)* **255,** 609–614.
12. Kraulis, P. J. (1991) *J. Appl. Crystallogr.* **24,** 946–950.
13. Eck, M. J. & Sprang, S. R. (1989) *J. Biol. Chem.* **264,** 17595–17605.
14. Jones, E. Y., Stuart, D. I. & Walker, N. C. P. (1989) *Nature (London)* **338,** 225–228.
15. Li, J., Carroll, J. & Ellar, D. J. (1991) *Nature (London)* **353,** 815–821.
16. Shimizu, T., Vassylyev, D. G., Kido, S., Doi, Y. & Morikawa, K. (1994) *EMBO J.* **13,** 1003–1010.
17. Finzel, B. C., Clancy, L. L., Holland, D. R., Muchmore, S. W., Watenpaugh, K. D. & Einspahr, H. M. (1989) *J. Mol. Biol.* **209,** 779–791.
18. Priestle, J. P., Schär, H.-P. & Grütter, M. G. (1989) *Proc. Natl. Acad. Sci. USA* **86,** 9667–9671.
19. Veerapandian, B., Gilliland, G. L., Raag, R., Svensson, A. L., Masui, Y., Hirai, Y. & Poulos, T. L. (1992) *Proteins Struct. Funct. Genet.* **12,** 10–23.
20. Zhu, X., Komiya, H., Chirino, A., Faham, S., Fox, G. M., Arakawa, T., Hsu, B. T. & Rees, D. C. (1991) *Science* **251,** 90–93.
21. Eriksson, A. E., Cousens, L. S., Weaver, L. H. & Matthews, B. W. (1991) *Proc. Natl. Acad. Sci. USA* **88,** 3441–3445.
22. Zhang, J. Cousens, L. S., Barr, P. J. & Sprang, S. R. (1991) *Proc. Natl. Acad. Sci. USA* **88,** 3446–3450.
23. Ago, H., Kitagawa, Y., Fujishima, A., Matsuura, Y. & Katsube, Y. (1991) *J. Biochem.* **110,** 360–363.
24. Cao, Y. & Petterson, R. F. (1993) *Growth Factors* **8,** 277–290.
25. Jessop, J. J. & Hoffman, T. (1993) *Lymphokine Cytokine Res.* **12,** 51–58.
26. Levitt, M. & Chothia, C. (1976) *Nature (London)* **261,** 552–558.
27. Rao, S. T. & Rossmann, M. G. (1973) *J. Mol. Biol.* **76,** 241–256.
28. Paralkar, V. & Wistow, G. (1994) *Genomics* **19,** 48–51.
29. Orengo, C. A. & Thornton, J. M. (1993) *Structure* **1,** 105–120.
30. Mizuguchi, K. & Go, N. (1995) *Protein Eng.* **8,** 353–362.
31. Steele, J. K., Kuchroo, V. K., Kawasaki, H., Jayaraman, S., Iwata, M., Ishizaka, K. & Dorf, M. E. (1989) *J. Immunol.* **142,** 2213–2220.
32. Murphy, D. B., Herzenberg, L. A., Okumura, K., Herzenberg, L. A. & McDevitt, H. O. (1976) *J. Exp. Med.* **144,** 699–712.
33. Tada, T., Taniguchi, M. & David, C. S. (1976) *J. Exp. Med.* **144,** 713–725.
34. Kronenberg, M., Steinmetz, M., Kobori, J., Kraig, E., Kapp, J. A., Pierce, C. W., Sorensen, C. M., Suzuki, G., Tada, T. & Hood, L. (1983) *Proc. Natl. Acad. Sci. USA* **80,** 5704–5708.
35. Cheah, E., Carr, P. D., Suffolk, P. M., Vasudevan, S. G., Dixon, N E. & Ollis, D. L. (1994) *Structure* **2,** 981–990.